Mine Water Environ (2016) 35:145–155
DOI 10.1007/s10230-015-0334-8

TECHNICAL ARTICLE

Groundwater Numerical Simulation in an Open Pit Mine in a Limestone Formation Using MODFLOW

José Paulino Fernández-Álvarez[1] · Lorena Álvarez-Álvarez[2] · Ramón Díaz-Noriega[2]

Received: 3 September 2014 / Accepted: 14 March 2015 / Published online: 26 March 2015

Abstract Numerical groundwater simulations of a complex limestone formation quarry in northern Spain enabled problems there to be quantified. A conceptual model of the aquifer, based on extensive in situ field work and information analysis was developed using MODFLOW. Steady state simulations as well as a first transient simulation were performed. The predictions matched the measured flows in the pit reasonably well, allowing practical scenarios of immediate interest to be simulated. Model calibration suggested a new permeability zonation, dependent of the degree of fracturing. The model provides a consistent quantitative framework with which new tests or operations can be evaluated in a cost effective manner.

Keywords Mining · Modeling · Hydrogeology · Water management

Electronic supplementary material The online version of this article (doi:10.1007/s10230-015-0334-8) contains supplementary material, which is available to authorized users.

✉ Lorena Álvarez-Álvarez
lorena@hydrogeophysicsndt.com

José Paulino Fernández-Álvarez
pauli@uniovi.es

Ramón Díaz-Noriega
ramon@hydrogeophysicsndt.com

[1] Department of Mines, Polytechnical School of Mieres, University of Oviedo, Gonzalo Gutiérrez Quirós s/n, 33600 Mieres, Asturias, Spain

[2] Hydrogeophysics and NDT Modelling Unit, University of Oviedo, Oviedo, Spain

Introduction

The application of numerical groundwater flow models to mining has increased considerably in the last few decades (Atkinson et al. 2010; Rapantova et al. 2007), especially for mine water management (Myers 2009; Rapantova et al. 2007) and for understanding the effects of mine subsidence on groundwater circulation patterns (Booth and Greer 2011). Groundwater numerical models are frequently used only as predictive tools, underestimating their power to integrate different types of data and cost effectively explore potential explanations of underlying physical processes (Brown and Trott 2014; Elango 2003). Used with this perspective, a model, such as MODFLOW (McDonald and Harbaugh 2003), may strongly suggest the collection of a certain kind of new data or provide new knowledge about mine operation parameters.

This article presents a numerical model of groundwater flow into an open pit mine. During wet seasons, the pit bottom floods because groundwater outflow exceeds the pumping capacity. With increasing quarry depths, the problem worsens, potentially threatening the feasibility of the mine. A more comprehensive understanding of the dynamics of the pit was desired, which led to us creating a numerical groundwater model in Visual Modflow. To parameterize the model, we built detailed digital topographical maps that reflected the evolution of the surface geometry of the quarry, after checking and digitizing the many heterogeneous pieces of already existing maps and transforming them to a common format. We also incorporated high resolution geology obtained from field work and analysis and correlation of 123 boreholes drilled by the company and additional data obtained by systematic analysis of the pumping network.

Characterization of the Study Area

The open pit limestone mine that we studied is located on the northern coast of Spain (Asturias). The extracted material constitutes a productive aquifer, so groundwater storage increases substantially during rainy periods, exceeding the installed pumping capability and flooding the deepest levels, disrupting production (Fig. 1). Adequate management of groundwater is critical and improving the knowledge of the contributing aquifers by means of a groundwater model was deemed important to optimizing long-term dewatering strategies.

The materials in the area are of Devonian and Carboniferous age, consisting primarily of sandstones and carbonates (limestone and dolomite). The sandstone formations generally have a very low permeability while some of the carbonate formations are karstic (Llopis Lladó 1970). The fractured, micritic Montana limestone is more than 300 m thick and is a highly permeable aquifer.

Tectonically, the study area is characterized by a large syncline fold with a north 70° east orientation and a periclinal closure at its southern side. The syncline measures about 6700 m along the symmetry axis of the fold and 1600 m in the perpendicular direction. The profile X–X′ shows a cross section of the fold along the axis (Fig. 2b). This main structure dips down to the northeast at an average angle between 2° and 4°, implying a thickening of the layers, particularly of the extracted Montana limestone formation, towards the east. The Hercynian orogeny (Beroiz et al. 1974) generated both this fold and a minor one with the same strike (at the right part of profile Y–Y′, Fig. 2c), which is important for local flows due to its intense fracturing. The Alpine orogenic phase caused a further longitudinal compartmentalization of the syncline. These faults appear in profile X–X′ as sub-vertical lines.

Field examination revealed three fracture systems: a family of tension fractures without displacement striking N40°W; a second that includes thrust faults parallel to the syncline axis, striking N125°W, which is responsible for a local thickening of the basin (see cross section X–X′ in Fig. 2b), where the quarry has better mining prospects; and a third family of half-moon faults striking N27 W in the NW limb and N30E in the SE limb. Taken together, there is a nearly uniform distribution of fractures that defines the small-scale representative elementary volume (R.E.V) in the Montana limestone formation, and explains its water conveying capacity. Given its consistent nature, it translates into a continuum porous medium model with an elevated equivalent permeability.

The opencast mine covers a surface area of 85×10^4 m^2 and by the date of this work, it had reached a maximum depth of −35 m below sea level (BSL). The typical mine geometry of batters (sloping walls) and benches can be seen in Fig. 1. It has evolved rapidly due to the mine's high

Fig. 1 Location **a** location of the watershed including the quarry; **b** deepest level flooded in winter; **c** evolving topography with batters and benches

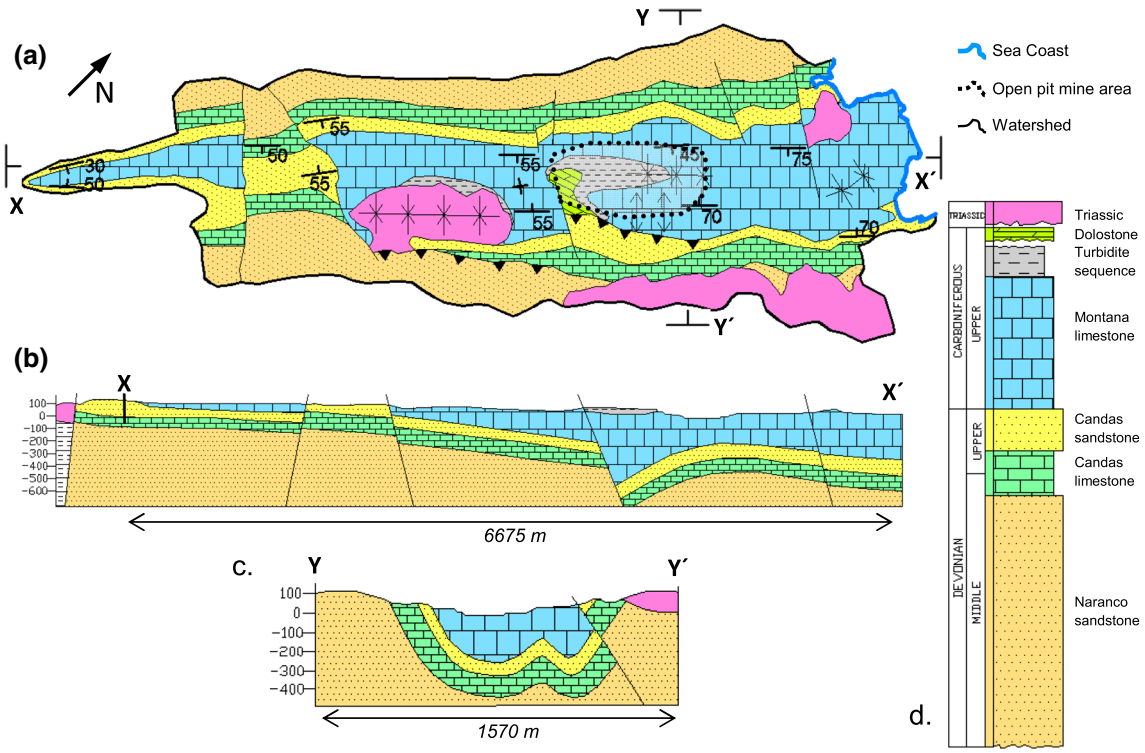

Fig. 2 Surface geological map, sequence, and cross sections **a** surface geological map showing the location of the open pit mine in the Montana limestone; **b**, **c** balanced vertical cross cuts in showing the internal general structure and tectonic features; **d** stratigraphical column with the main formations present in the area

extraction rate, producing an annual volume change of 15 %. The slopes are usually kept around 72°, with benches approximately 18 m high. The limestone strata is broken by conventional blasting that increases fracturing near the active area.

The changing geometry of the quarry was assessed by analysis of topographical maps and aerial photographs of the quarry from 1991 to the present. These maps were carefully checked, digitized, and transformed into a common format for their use in this work. Detailed in situ geological field work was also carried out to build the conceptual model. The resulting stratigraphic column can be seen in Fig. 2d.

The cartographic map of Fig. 2 includes the results of analyzing 123 boreholes, showing lithologies and depths to contacts, which were also systematized and georeferenced for further use. Seven of the wells drilled through the limestone achieved a maximum depth of 100 m BSL, showing that the limestone extends at least 65 m below the mine bottom (−35 m BSL). The maximum depth estimates were derived from the balanced cross sections, assuming: volume conservation, that only the mentioned tectonic structures were present, and consistency among the bed lengths unless a discontinuity had to be considered, based on collected field data (Dahlstrom 1969).

Description of Hydrological Data

Meteorological data were obtained from six nearby weather stations, which provided precipitation and temperature time series data. As there were time gaps, cross-correlation was used to form a unique complete precipitation time series from the 1930s until the present that could be applied to the study area. For use in the stationary model, an average precipitation rate of 941.5 mm/year was obtained, with maxima and minima of 1303.2 and 537.1 mm/year, respectively. These bounds were also used in simulating the different scenarios.

The evapotranspiration was calculated directly from the meteorological data previously described using the formula of Le Turc (Maidment 1992). The average evapotranspiration value was 55 % of the precipitation, with upper and lower bounds of 70 and 40 %.

The input recharge area was derived from the field work performed on the hydrology of the study area as 10.59×10^6 m^2, delimited by the watershed divide and the sea border. The stream system has a total length of about 12 km; careful differential gauging was performed to quantify surface runoff and infiltration (Fig. 3).

A total of 67 water points were inventoried, consisting of springs, wells, and boreholes, of which only 9 were used

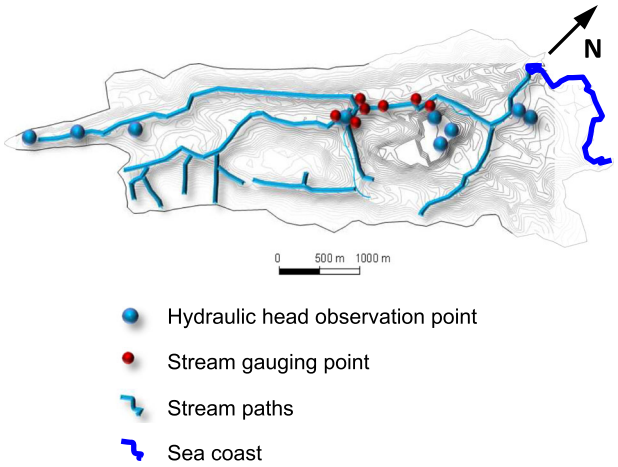

Fig. 3 Hydrological information shows the stream network and its gauging points

for monitoring of hydraulic heads (Fig. 3) in the steady state model because of their location in the main aquifer (Montana limestone) and accessibility. For each water point, an associated file was created, with its location, photographs, geological and hydrogeological characteristics, observations, and measurements. The water recharge to the aquifer had an average value of 542.6 mm/year, with 1019.7 and 161.1 mm/year, being the lower and upper bounds, respectively.

Groundwater outflow to the pit was quantified from the pumps of the installed dewatering system, after subtracting the surface runoff, calculated from the river gauging data. The drainage system comprises a pump system and engineered ponds that are used to regulate discharges (Supplemental Fig. 1). [Supplemental figures and tables accompany the on-line version of this paper, which can be downloaded for free by all journal subscribers and IMWA members.] The field work identified permanent localized groundwater outflows where local hydrographs, correlated with the rain events, showed very short residence times (<3 days).

Discussion of the Conceptual Model

The main aquifer body is the Montana limestone formation. The initial goal was to find a framework that consistently fit the existing information. It seemed reasonable to first focus on average annual pit outflows and heads and analyze the permanent regime. A preliminary subsequent transient analysis matched the time evolution of the global flows to the pit and further constrained the aquifer characteristics.

Different hydraulic conductivity values were assigned for each layer of the model. The Montana limestone formation was first assumed to be homogeneous and a steady model was run to fit the global discharge in the quarry. Afterwards, a new zonal heterogeneous model was developed that matched the spatial distribution of localized flows in the pit.

The evolving geometry might suggest the use of time-dependent boundary conditions. However, the geometry is only updated in December of each year and, in later years, including those studied here, the increased groundwater inflow to the pit has slowed down the production rate, so that the geometry does not change so quickly. Therefore, the available geometry was assumed to be a valid average of the situation of each year.

Part of the field work was focused on identifying the role that the larger faults played in groundwater circulation. However, no evidence was found in favor of conductive faults; instead, the fractures are localized and disappear before reaching the bottom of the Naranco sandstone formation. So, individual fractures are not currently included in this model but could be incorporated if any of them are found to be significant.

Field inspection of the exposed aquifer uncovered by mining revealed the existence of small voids and fissures (enhanced by the effect of the explosives) that will certainly convey water locally in a non-Darcian manner. However, since the goal of the model was to integrate the spatial scale of the entire formation, the fractured limestone aquifer was replaced by an equivalent continuum characterized by an effective hydraulic conductivity (Bear 1972).

The boundaries of the model at the surface coincide with the topographic watershed line. Infiltration out of this line would have to take place in the Naranco Sandstone formation or in parts of the Triassic formation, both of which were considered highly improbable. The groundwater flows towards the Montana limestone. The underground boundaries of the model follow the bottom of the Naranco sandstone formation. Many of its members are considered to be impermeable along its half kilometer thickness in the area. Hypothetical tension fractures developed at its bottom, linked to the syncline curvature, would not be connected to each other. This was translated into a Neumann no-flow boundary condition.

Areal recharge is directly input at the surface where the limestone outcrops and the net precipitation almost entirely enters the aquifer. The stream system conveys water from runoff. Infiltration data for the stream reaches are available from the differential gauges carried out during the survey and from observation of the stream behavior during the hydrologic year. A specified flow was used to characterize the stream-aquifer interaction.

The coast line is around 1100 m from the quarry. The sea water contact is simulated as a Dirichlet boundary condition, being a constant head equal to the mean sea level. Density differences between the sea water and the

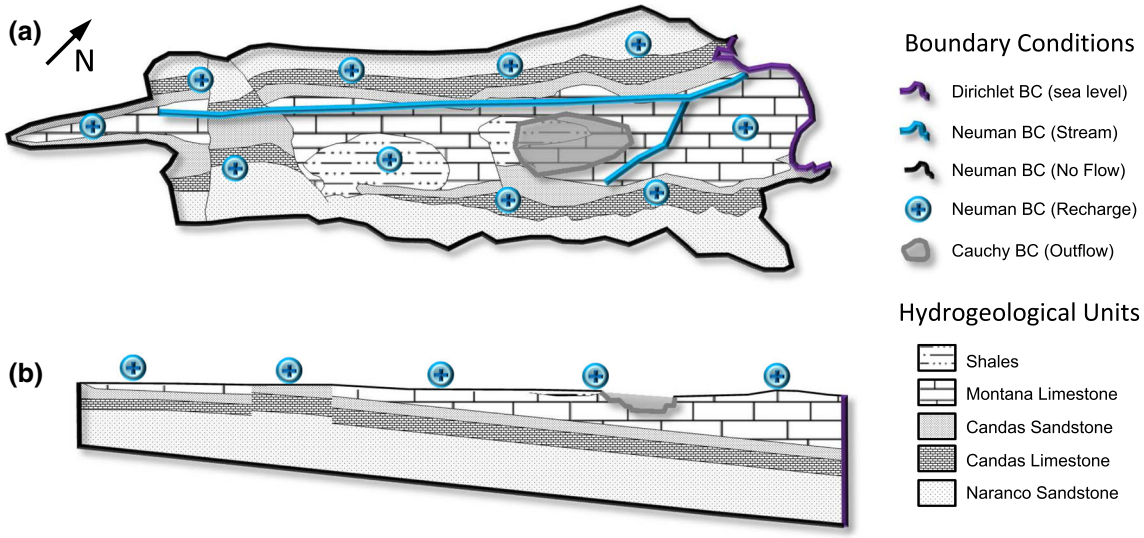

Fig. 4 Conceptual model: **a** plan view of the different boundary conditions employed; **b** vertical cross section showing boundary conditions and the hydrogeological units present

fresh water are not considered in this first model (Fig. 4a, b). The outflow of water to the quarry through the surface of the batters was simulated using a boundary condition of the third type in MODFLOW.

Model Design

The numerical implementation was carried out based on this conceptual model using Visual MODFLOW, which is a finite difference computer code commercialized by Schlumberger (Schumberger Water Services 2009). The outer surface of the benches in the active mining front was modeled using a third type boundary condition. The conductance factor needed was set according to the expected permeability of the zone and the dimensions of the cells; the required reference level was set equal to the topographic elevation of that point. With these specifications, the water leaving the model mimics the groundwater discharge through the mined faces.

The MODFLOW spatial discretization used a rectangular grid with 158 rows, 380 columns, and 21 numerical layers along the vertical dimension. The average size of the cell was 25 m and was refined by a factor of 4 in the quarry region to accurately represent the complex geometry of batter and benches and its evolution with time. This version of MODFLOW required the extension of each refined column or file to the boundary of the model, which is clearly superfluous. A local refining strategy would be more economic computationally and there are new versions available that enable local refinement (Krčmář and Sracek 2014).

For the transient simulation, the same grid was employed and the code was run for a 1 year period, from May 2010 to April 2011, where flow measurements were available. Each stress period corresponded to 1 month and recharge was recalculated monthly. The hydraulic conductivity values are shown in Fig. 5, together with the finite difference mesh. The groundwater outflow to the quarry, both in steady state and in the transient simulations, was obtained by setting a water budget zone in the boundary condition cells or elements surrounding it.

Parameter Estimation, Sensitivity Analysis and Model Verification

Following the modeling protocol (Anderson and Woessner 1991), a steady state parameter estimate was performed once the conceptual model was implemented. The model was then calibrated to give it the ability to reproduce a certain family of collected field measurements (Carrera et al. 2005). A first calibration was done based on the hydraulic conductivity values for a homogeneous limestone model, using the average measured total groundwater flow to the quarry during the period between May 2010 and April 2011 and the water head in the six wells shown in Fig. 6 as data. The model was run using average values of precipitation and evapotranspiration.

A careful assessment of the drainage pumping network established that the empirical standard deviation was 15 % for the measured flows and 3 % for the measured water levels available. These figures were used as threshold tolerances. Any model achieving a root mean square (RMS)

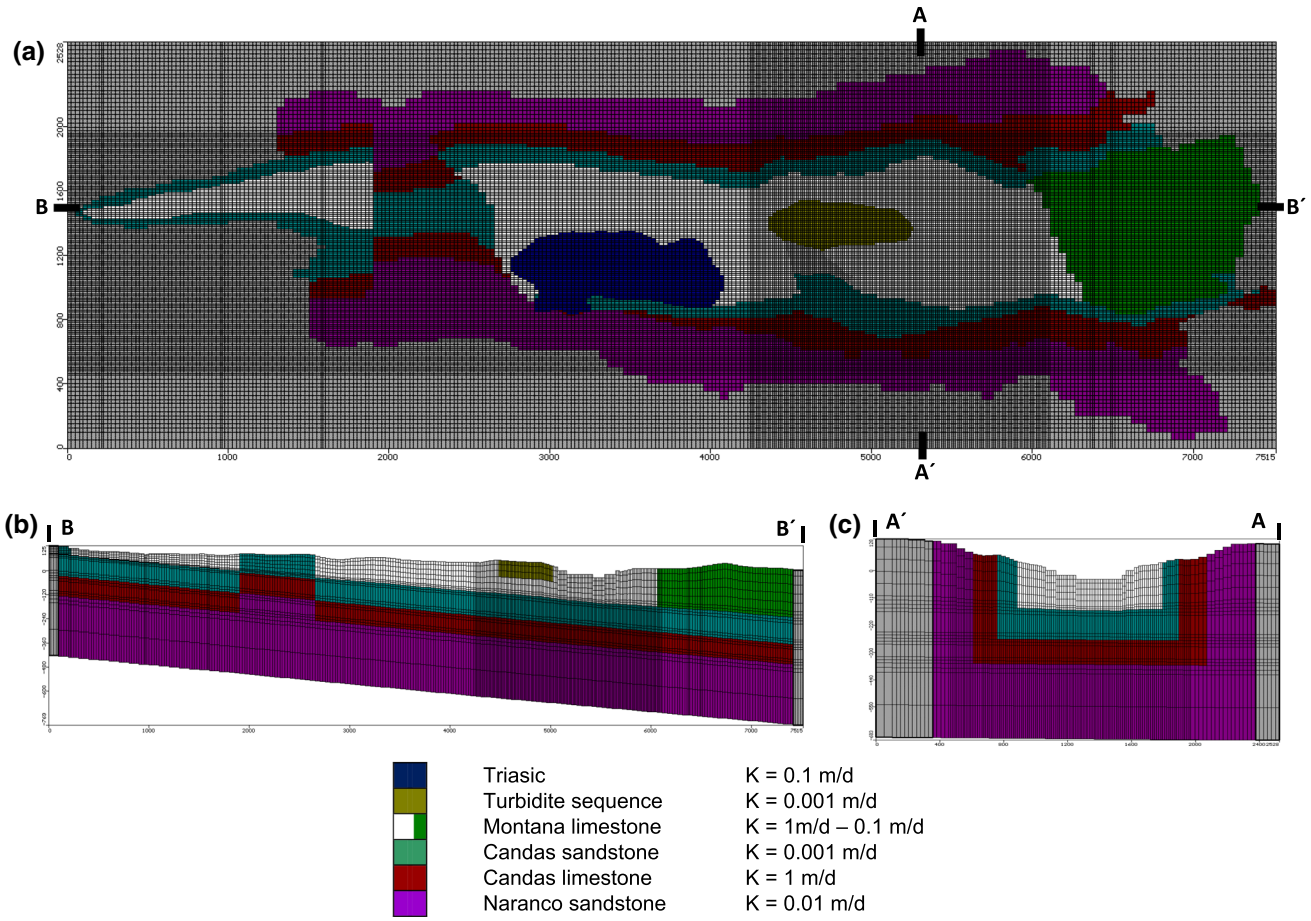

Fig. 5 Model discretization; **a** mesh in plan view; **b** longitudinal cut showing the mesh and the hydrogeological units; **c** transversal cross section. The values shown are estimated

discrepancy between predicted and measured values below them was considered acceptable. Calibration was done by trial and error; no automatic estimation method was used. The parameters of the homogeneous model are shown in Fig. 5. The data and the quality of fit are shown in Fig. 6 for those estimated values. Other equivalent models are possible, as explained later.

However, the mine geometry for the considered period differed from that of 2013 when analysis of predictive scenarios was needed and from that of 2003, which was used for retro-validation. Modeling geometries were therefore modified accordingly.

The geological study also detected various highly fractured zones. Some of these were able to transmit water with a delay time of 3 days, based on correlations with in situ measured values. Although the simulation performed using a single hydraulic conductivity value for the limestone provided results consistent with the global outflow to the pit, it does not honor these localized flow measurements. Therefore, a permeability zonation was introduced that better matches the anomalous local flows, supporting the existence of a higher permeability area inside the area of active dewatering for quarry operations. The hydraulic conductivity of the new zones was 1000 m/day near the river and 100 m/day along the anticline axis (Fig. 7).

A transient simulation was later performed, starting with the stationary model. Predicted monthly outflows to the pit were compared with the measured monthly global flows. Time evolution of observed water heads was not available. Figure 8 and supplemental Table 1 show how the fit captures the seasonal variation and matches the values, within the 15 % tolerance of the measurements.

Different models were able to produce misfits under the required tolerances. Equivalent models were obtained by simultaneously changing the conductivity and the thickness of the limestone formation. In Fig. 9, the limestone thickness was varied using limestone permeability as a parameter. The feasible portion is vertically bounded by geologic estimations (red lines) and horizontally by the value of the tolerance misfit value (blue lines). The two vertical lines represent the lower bound for the limestone thickness obtained from the already drilled boreholes,

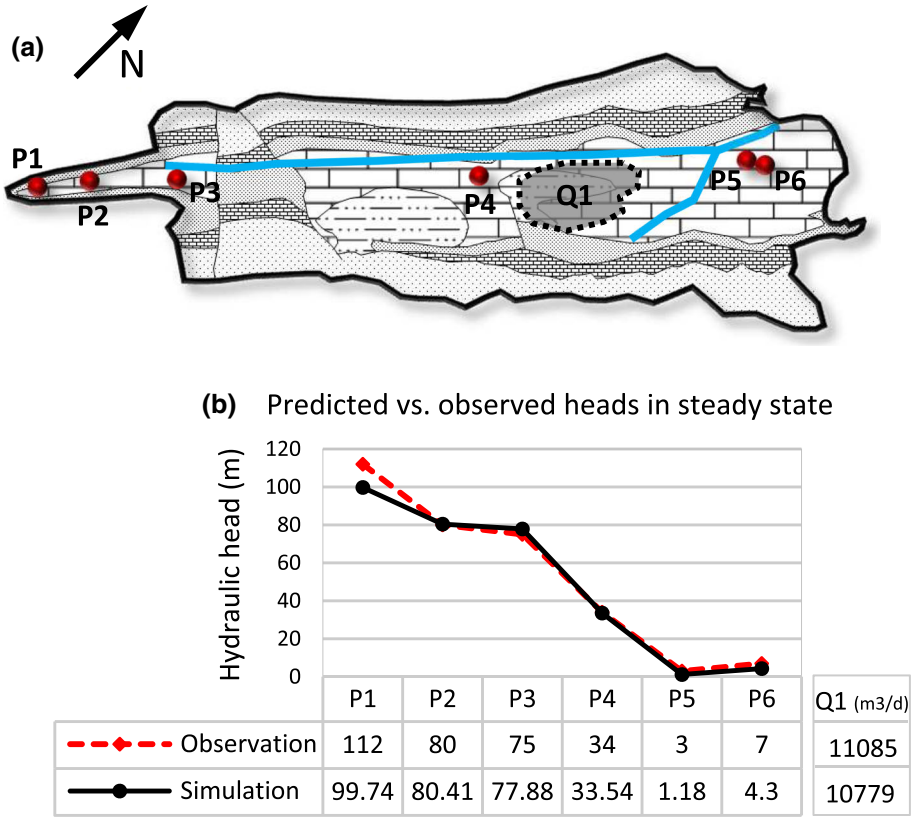

Fig. 6 Location of observation points: **a** situation of the head observation points and outflow to the pit; **b** observed values and fit; root mean square (RMS) = 2.18 m

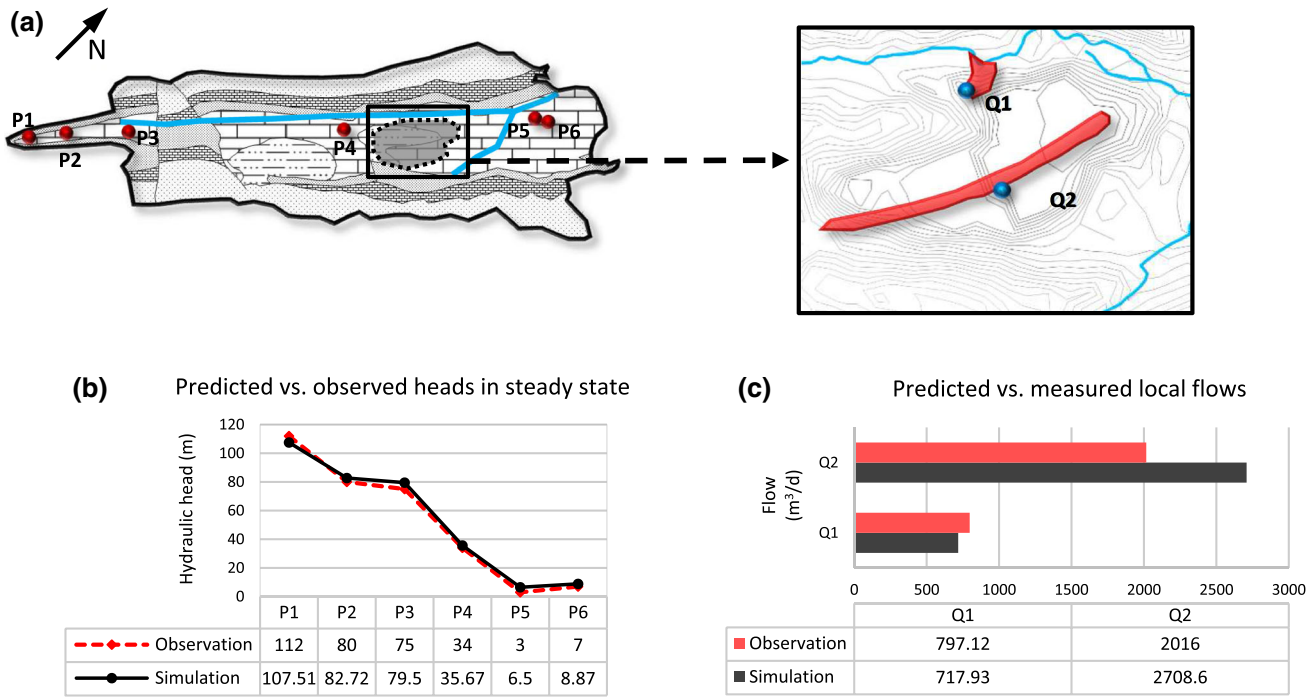

Fig. 7 Permeability zonation: **a** detailed view of the local flows measured in the pit and the high permeability zones included in the model to better fit them; **b** fit between observed and predicted heads (RMS = 3.3 m); **c** fit between predicted and measured local flows

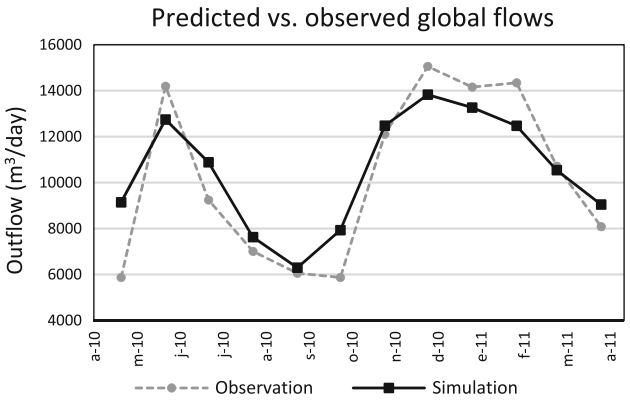

Fig. 8 Predicted versus observed global flows graph with observed and predicted values of total monthly outflow (RMS = 14.6 %). Numerical data in supplemental Table 1

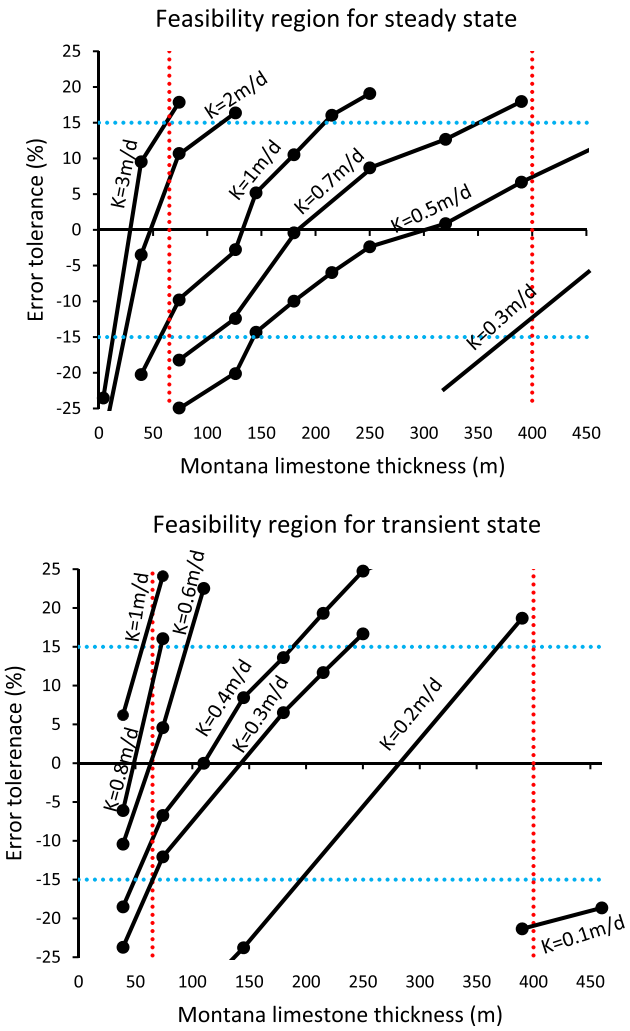

Fig. 9 Feasibility regions: **a** feasibility region obtained from steady state knowledge; **b** feasibility region obtained from the preliminary transient simulation. Note that values of K over 0.8 m/day have become infeasible

whereas the upper bound was obtained from geological interpretation. A conductivity from 0.3 to 2 m/day was considered permissable. Reversing the argument, a maximum thickness for the limestone would be obtained given any reliable conductivity value. For instance, for k = 0.3 m/day, the maximum thickness would be 235 m.

Figure 9b shows how the non-uniqueness of the parameters attributed to the limestone was reduced. The new feasibility area imposes a maximum hydraulic conductivity of 0.8 m/day. This gives a clear context that shows the immediate usefulness of pumping tests and graphically summarizes the level of knowledge contained in the data used for the steady state simulation.

A sensitivity analysis was performed for different numerical aspects of the problem under study. For instance, the influence of the mesh grid, both horizontally and vertically, was assessed, looking to optimize the easiness of convergence and the computation time while achieving acceptable residual balances.

The parameters determined in the calibration phase were used to (back) predict the pit outflows in 2003, the only one in the past for which the data were considered reliable enough, albeit with a different (smaller) affected geometry. The difference between the average measured and predicted result was 13 %. Therefore, the models were deemed sufficient to incorporate further information and perform hypothesis analysis.

Discussion of Different Scenarios of Practical Interest

Once the model is further refined and capable of consistently integrating the measured data and conceptual model, it will be employed to gain insight into some characteristics of hypothetical scenarios of practical interest. Among the feasible family of values, simulations have been run with the following representative values for illustration purposes: 0.5 m/day for limestones (Montana and Candas), 10^{-1} m/day for Triassic materials and Montana limestone in Peran place, 10^{-2} m/day for dolostone and Naranco sandstone, and 10^{-3} m/day for the turbidite sequence and Candas sandstone. Although the actual model does not handle density dependent flow, considered to be too sophisticated at this stage for the actual quantity and quality of the data, the existence and position of the groundwater divide might be used with caution to preliminarily assess the risk of a sea water intrusion reaching the pit as the quarry is deepened as planned. At present, there is empirical evidence of fresh water discharge at localized points at the sea coast, so no intrusion is taking place. But this situation might change for different scenarios such as:

Scenario 1

Estimated lower and upper bounds for the outflow with the pit's current geometry. Estimates were obtained by running models using the appropriate combination of upper and lower limits for precipitation (1303.2 and 537.1 mm/year) and evapotranspiration (70 and 40 %), together with bounds of stream infiltration measured by differential gauging (6900 and 0 m^3/day). The predicted variations would be interpretable as limiting feasible events as long as the quarry geometry is considered to be invariant. The maximum pit outflow would be 49 % greater and the minimum would be 62 % less than the average actual prediction (see Fig. 10). The groundwater divide moves accordingly and, for the lowest values case, suggests that attention should be paid to the possibility of intrusion.

Scenario 2

To decrease the amount of leakage of water from the stream, partial channeling was envisaged for the reach traversing the company's property. This channeling scenario, once modeled suppressing the recharge at the modified reach and using average recharge values everywhere else, predicted a 24 % reduction in groundwater flow at the bottom pit (Supplemental Fig. 2).

Scenario 3

Shows the prediction of the average pit outflow for the projected geometry for year 2020. Here, an average recharge value of 423.7 mm/year and stream infiltration of 3450 m^3/day were used as input. The depth of the new open face is now 53 m below sea level and the predicted

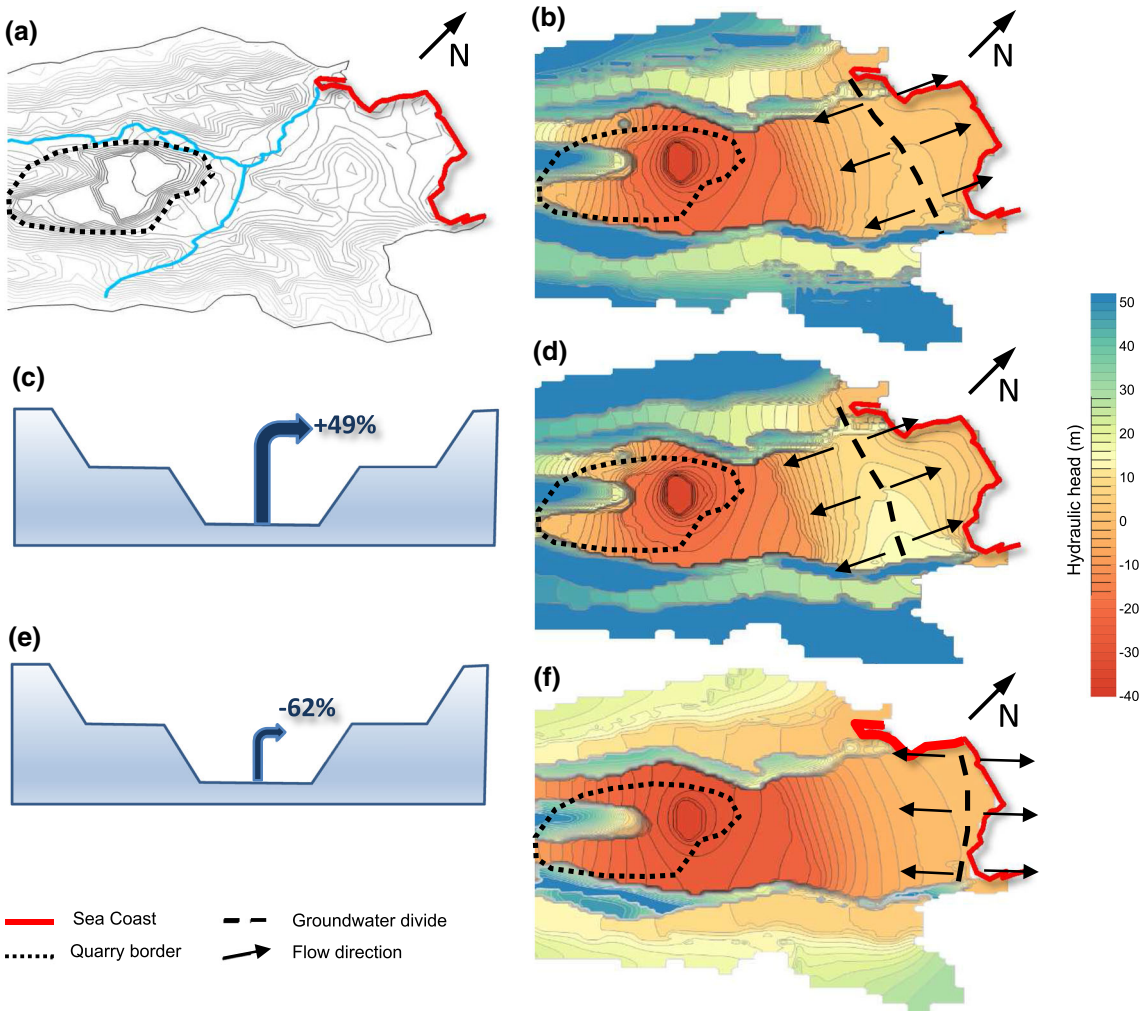

Fig. 10 Scenario 1: **a** situation map showing the quarry, the coast line and the rivers; **b** piezometric map of the limestone aquifer for the average situation. The *dashed line* represents the position of the groundwater divide; **c**, **d** show the case when the upper limit is used. The groundwater divide is slightly displaced and deformed to the south (*left*) and the outflow to the pit increases by 49 %. **e**, **f** the lower bounds are used and the groundwater divide shifts to very close to the coast. Discharge to the pit is 62 % less than the average

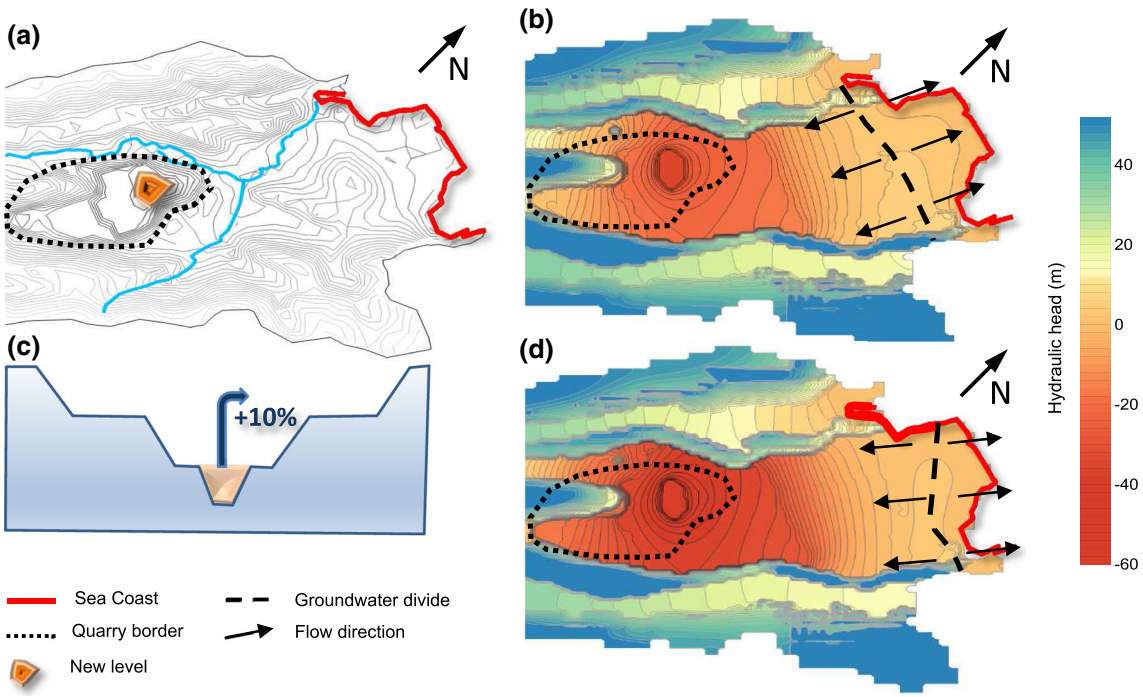

Fig. 11 Scenario 3: **a** shows the new future level of the pit; **b** piezometric map and position of the groundwater divide in the limestone aquifer for the average situation; **c**, **d** the impact of the future mining plan is important; it not only increases the pumping needs by 10 %, but produces an important shift in the groundwater divide

pumping capacity should be increased by 10 % (Fig. 11). Given the observed displacement of the groundwater divide, a more detailed study of a possible sea water intrusion is recommended for scenario 3.

Conclusions

Groundwater models are useful in integrating different types of data into a consistent framework, rendering the information useful and interpretable. In open mine pit exploitations where the extraction rate and production times are the dominant economic factor, specialized hydrogeologic tests and continuous monitoring are unusual. This paper shows how a numerical model was used to integrate existing data of different qualities in a consistent way. This provided a framework that indicated how results should be refined through further experiments and proved useful to mine management departments concerned with production and safety. The practical scenarios developed above illustrate the potential value of the model.

Acknowledgments The authors thank the two anonymous reviewers for their detailed comments and suggestions that greatly improved this article.

References

Anderson MP, Woessner WW (1991) Applied groundwater modeling: simulation of flow and advectivetransport. Academic Press, San Diego

Atkinson LC, Keeping PG, Wright JC, Liu Houmao (2010) The challenges of dewatering at the Victor Diamond Mine in northern Ontario, Canada. Mine Water Environ 29(2):99–107. doi:10.1007/s10230-010-0109-1

Bear J (1972) Dynamics of fluids in porous media. Elsevier, New York

Beroiz C, Ramirez del Pozo J, Giannini G, Barón A, Julivert M, Truyols J (1974) Memoria Magna Hoja 0014 (Gijón). Magna Memory Page 0014 (Gijón). http://info.igme.es/cartografia/magna50.asp?hoja=14&bis= (in Spanish)

Booth CJ, Greer CB (2011) Application of MODFLOW using TMR and discrete step modification of hydrulic properties to simulate the hydrogeologic impact of longwall mining subsidence on overlying shallow aquifers. Proc, Mine Water—Managing the Challenges, Aachen, Germany, pp 211–215

Brown K, Trott S (2014) Groundwater flow models in open pit mining: can we do better? Mine Water Environ 33(2):187–190. doi:10.1007/s10230-014-0270-z

Carrera J, Alcolea A, Medina A, Hidalgo J, Slooten LJ (2005) Inverse problem in hydrogeology. Hydrogeol J 13(1):206–222. doi:10.1007/s10040-004-0404-7

Dahlstrom CDA (1969) Balanced cross sections. Can J Earth Sci 6:743–757. doi:10.1139/e69-069

Elango L (2003) Numerical modelling—an emerging tool for sustainable management of aquifers. J Appl Hydrol XVIII(4):40–46

Krčmář D, Sracek O (2014) MODFLOW-USG: the new possibilities in mine hydrogeology modelling (or what is not written in the

manuals). Mine Water Environ 33(4):376–383. doi:10.1007/s10230-014-0273-9

Llopis Lladó N (1970) Fundamentos de Hidrología Cárstica (foundations of karst hydrology). Blume, Madrid

Maidment DR (1992) Handbook of hydrology. McGraw-Hill Handbooks, New York

Mcdonald MG, Harbaugh AW (2003) The history of MODFLOW. Ground Water 41(2):280–283. doi:10.1111/j.1745-6584.2003.tb02591.x

Myers T (2009) Groundwater management and coal bed methane development in the Powder River Basin of Montana. J Hydrol 368(1–4):178–193. doi:10.1016/j.jhydrol.2009.02.001

Rapantova N, Grmela A, Vojtek D, Halir J, Michalek B (2007) Ground water flow modelling applications in mining hydrogeology. Mine Water Environ 26(4):264–270. doi:10.1007/s10230-007-0017-1

Schumberger Water Services (2009) Visual MODFLOW user's manual. http://trials.swstechnology.com/archive/Software/VMOD/2009.1/VisualMODFLOW_2009.1_UsersManual.pdf